Inducing Pendant Group Interactions in Precision Polyolefins: Synthesis and Thermal Behavior

Erik B. Berda and Kenneth B. Wagener*

The George and Josephine Butler Polymer Research Laboratory, Department of Chemistry, University of Florida, Gainesville, Florida 32611-7200

Received March 19, 2008; Revised Manuscript Received May 22, 2008

ABSTRACT: The synthesis and thermal behavior of polyethylene with precisely placed amphiphilic branches are described. The amphiphilic branches contain tetraethylene glycol as the hydrophilic segment and either pyrene, *n*-hexyl, or *n*-tetradecyl moieties as the hydrophobic segment. Monomer and precursor structures have been confirmed by ^{1}H and ^{13}C NMR, elemental analysis, and high-resolution mass spectrometry. The structures of the corresponding polymers have been confirmed by ^{1}H NMR, ^{13}C NMR, and FTIR. Differential scanning calorimetry (DSC) and temperature-modulated DSC (MDSC) were used to study the behavior of these materials in the bulk. The branch distribution was kept constant to probe the effect of changing the hydrophobic graft end group. Altering this group produced significant changes in the observed thermal behavior, implying completely different morphologies for these materials. When the graft end group is a pyrene moiety, the polyolefin backbone crystallizes excluding the pendant branch, which aggregate as confirmed by fluorescence measurements. When this end group is changed to an *n*-hexyl chain, the branches and the backbone crystallize separately, forming two different crystalline regions. Extending this end group from an *n*-hexyl to an *n*-tetradecyl chain allows the branches and backbone to crystallize together, resulting in the inclusion of the branch within the crystal. This material deviates from the well-known trend for ADMET polymers, which show a decrease in melting temperature and enthalpy as the defect size increases.

Introduction

It is well understood that highly regular macromolecular structures result in predictable and controllable material behavior. This is especially true with amphiphilic copolymers, for which minor alterations in structure can induce a broad range of responses in the bulk and in solution.[1–5] The amount of research on the synthesis and self-assembly of amphiphilic block copolymers alone is remarkable.[5–11] Living radical,[9,12] cationic,[8,13] anionic,[14] and even metathesis[15] polymerizations have been extensively utilized in creating well-defined structures that can self-assemble to form interesting and useful morphologies.

The use of acyclic diene metathesis (ADMET) to create highly regular, precisely defined structures is also well-known.[16–18] These materials, while often structurally related to copolymers made via chain copolymerization of ethylene and vinyl comonomers, possess properties that distinguish them as a completely separate class of materials.[16,19–28] These properties are highly tunable with minor structural alterations, imparted during the synthesis of the symmetrical terminal diolefin monomer. Two parameters are generally altered: the identity of the pendant functional moiety and the static methylene sequence length between this functional group and the terminal olefin. When the pendant moiety is a methyl group, systematically changing the methylene sequence length from branches every seventh carbon to branches every 21st carbon results in a control of melting point over a range of 200 °C.[27,29] Likewise, alteration of the pendant group size and polarity allows tunability of the properties when the methylene sequence length is held constant. In all ADMET copolymers observed previously, an increase in defect size results in a systematic decrease in melting temperature.[21,22,26]

A recent area of research in our group has been the use of ADMET to synthesize a family of amphiphilic graft copolymers with polyethylene (PE) backbones and hydrophilic poly(ethylene glycol) (PEG) branches. By combining the structural regularity available with ADMET and the ability of amphiphiles to phase separate and self-assemble, we have created semicrystalline materials in which the PE backbone crystallizes, forming pure hydrocarbon crystallites excluding the polyether branches.[30] We expand this area of research in this report by altering the pendant PEG chain end group to create copolymers with PE backbones and AB amphiphilic grafts. Two of the polymers reported have the A-*g*-(B-*b*-A) motif, where an oligoethylene chain is affixed to the end of the PEG branch directly attached to the PE backbone. The third has a pyrene group attached to the end of the PEG chain. Labeling in the fashion allows the aggregation of these graft end groups to be examined using fluorescence measurements. To assess the influence of these pendant groups on the PE backbone accurately, the distance between pendant groups was kept constant in this study. To ensure the crystallization of the backbone, a 21-carbon distance between pendant branches was chosen because previous ADMET polymers with this functional group distribution have always been semicrystalline.[16–18]

All monomer and precursor structures were confirmed by ^{1}H and ^{13}C NMR, elemental analysis, and high-resolution mass spectrometry. The structures of the corresponding polymers were confirmed by ^{1}H NMR, ^{13}C NMR, and FTIR. Differential scanning calorimetry (DSC) and temperature-modulated DSC (MDSC) were used to study the behavior of these materials in the bulk. The observed thermal behavior indicates that the three materials have very different morphologies. Affixing the PEG branch with a pyrene end group results in the complete exclusion of the pendant moiety from the crystal. Changing the end group to an *n*-hexyl chain results in crystallization of the pendant branch separately from the PE backbone. Extending this oligoethylene chain from *n*-hexyl to *n*-tetradecyl allows the pendant moiety to extend back into the polymer crystal, thereby increasing the melting point compared to the polymers with the six-carbon terminus. The inclusion of the PEG-*b*-tetradecyl group into the crystal is significant because it breaks the usual trend for ADMET polymers, which show a decrease in melting point and melting enthalpy with increasing pendant group size.

* Corresponding author. E-mail: wagener@chem.ufl.edu.

10.1021/ma800616h CCC: $40.75
Published on Web 06/21/2008

Experimental Section

Instrumentation. All ^{1}H NMR (300 MHz) and ^{13}C NMR (75 MHz) spectra were recorded on a Varian Associates Mercury 300 spectrometer. Chemical shifts for ^{1}H and ^{13}C NMR were referenced to residual signals from $CDCl_3$ (^{1}H: $\delta = 7.27$ ppm; ^{13}C: $\delta = 77.23$ ppm) with 0.03% (v/v) TMS as an internal reference. Thin layer chromatography (TLC) was performed on EMD silica gel-coated (250 μm thickness) glass plates. Developed TLC plates were stained with iodine adsorbed on silica to produce a visible signature. Reaction conversions and relative purity of crude products were monitored by TLC and ^{1}H NMR. Fourier transform infrared (FT-IR) measurements were conducted with a Bruker Vector 22 infrared spectrophotometer using polymer films cast from chloroform onto KBr plates. High-resolution mass spectrometry analyses were performed on a Bruker APEX II 4.7 T Fourier transform ion cyclotron resonance mass spectrometer (Bruker Daltonics, Billerica, MA) using electrospray ionization (ESI). Elemental analysis was carried out at Atlantic Microlab Inc. (Norcross, GA).

Molecular weights and molecular weight distributions (M_n/M_w) were determined by gel permeation chromatography (GPC) using a Waters Associates GPCV2000 liquid chromatography system with an internal differential refractive index detector (DRI) and two Waters Styragel HR-5E columns (10 μm particle diameter, 7.8 mm i.d., 300 mm length) at 40 °C. The mobile phase was HPLC grade tetrahydrofuran at a flow rate of 1.0 mL/min). Retention times were calibrated vs polystyrene standards (Polymer Laboratories, Amherst, MA).

Differential scanning calorimetry (DSC) and temperature-modulated differential scanning calorimetry (MDSC) were performed on a TA Instruments Q1000 equipped with a liquid nitrogen cooling accessory calibrated using sapphire and high-purity indium metal. All samples were prepared in hermetically sealed pans (4−7 mg/sample) and were referenced to an empty pan. A scan rate of 10 °C/min was used unless otherwise specified. Modulated experiments were scanned with a 3 °C/min linear heating rate with modulation amplitude of 0.45 °C and period of 30 s. Melting temperatures are taken as the peak of the melting transition and glass transition temperatures as the midpoint of a step change in heat capacity.

Materials. Unless otherwise stated, all reagents were purchased from Aldrich and used without further purification. Grubbs' first generation catalyst was a gift from Materia, Inc. Diene alcohol **1** was synthesized as previously reported.[25]

Synthesis of 2-(10-Undecenyl)-12-tridecenyl-1-tetra(ethylene glycol) *p*-Tosylate (2). Anhydrous DMF (30 mL) was cannula transferred into an oven-dried, three-neck round-bottom flask equipped with a magnetic stirrer and gas inlet and was charged with 2 equiv of sodium hydride (60% dispersion in mineral oil). The slurry was cooled to 0 °C, and 1 equiv of **1** in 20 mL of anhydrous DMF was added via syringe. When hydrogen gas evolution (monitored by bubbler) ceased, the solution was cannula transferred into a well-stirred flask containing 4.5 equiv of tetraethylene glycol di-*p*-tosylate in 50 mL of anhydrous DMF. The reaction was stirred for 17 h at 0 °C and quenched by pouring into 300 mL of water. The resulting mixture was extracted with diethyl ether, and the combined organics were washed with brine. Concentration afforded a yellow oil which was further purified by column chromatography, 30% ethyl acetate and 70% hexane eluent, yielding 1.5 g (52%) of colorless oil. ^{1}H NMR ($CDCl_3$): δ (ppm) 1.21−1.52 (br, 33H), 2.01 (q, 4H), 2.42 (s, 3H), 3.29 (d, 2H), 3.50−3.75 (br, 15H), 4.18 (d, 2H), 4.98 (m, 4H), 5.82 (m, 2H), 7.31 (d, 2H), 7.79 (d, 2H). ^{13}C NMR ($CDCl_3$): δ (ppm) 21.82, 27.01, 29.15, 29.35, 29.70, 20.80, 29.83, 30.28, 31.55, 34.00, 38.32, 68.89, 69.39, 70.57, 70.74, 70.79, 70.80, 70.88, 70.97, 75.01, 114.28, 128.18, 129.99, 133.33, 139.43, 144.92. ESI/HRMS: $[M + NH_4]^+$ calcd for $NH_4C_{39}H_{68}O_7S$, 698.5024; found 698.5023. Anal. (CH) calcd for $C_{39}H_{68}O_7S$: C, 68.78; H, 10.06. Found: C, 58.51; H, 9.95.

General Procedure for Preparation of Monomers. Anhydrous DMF (45 mL) was cannula transferred into an oven-dried, three-neck round-bottom flask equipped with a magnetic stirrer and gas inlet and was charged with 2 equiv of sodium hydride (60% dispersion in mineral oil). The slurry was cooled to 0 °C, and **3** was added in 20 mL of anhydrous DMF via syringe. When hydrogen gas evolution (monitored by bubbler) ceased, 1 equiv of **2** in 30 mL of anhydrous DMF was added via syringe. The reaction was stirred for 17 h at 0 °C and quenched by pouring into 300 mL of water. The resulting mixture was extracted with diethyl ether, and the combined organics were washed with brine. Concentration afforded a yellow oil which was further purified by column chromatography.

2-(10-Undecenyl)-12-tridecenyl-1-tetra(ethylene glycol)methenylpyrene (9,9TEGOPy, 3a). 30% ethyl acetate and 70% hexane eluent afforded 0.475 g (29% yield) of colorless oil. ^{1}H NMR ($CDCl_3$): δ (ppm) 1.21−1.52 (br, 33H), 2.01 (q, 4H), 3.29 (d, 2H), 3.50−3.75 (br, 12H) 4.98 (m, 4H), 5.28 (s, 2H), 5.82 (m, 2H), 7.61−8.79 (m, 4H), 8.13−8.20 (m, 4H), 8.37 (d, 1H). ^{13}C NMR ($CDCl_3$): δ (ppm) 26.96, 29.14, 29.35, 29.71, 20.82, 29.85, 30.28, 31.52, 34.01, 38.28, 69.72, 70.54, 70.75, 70.83, 70.87, 70.95, 72.04, 74.96, 114.28, 123.75, 124.64, 124.92, 125.36, 126.09, 127.22, 127.60, 127.83, 131.03, 131.47, 131.62, 139.43. ESI/HRMS: $[M + NH_4]^+$ calcd for $NH_4C_{49}H_{72}O_5$, 758.5718; found 758.5735. Anal. (CH) calcd for $C_{49}H_{72}O_5$: C, 79.41; H, 9.79. Found: C, 79.00; H, 9.80.

2-(10-Undecenyl)-12-tridecenyl-1-tetra(ethylene glycol) Mono-*n*-hexyl Ether (9,9TEGOHex, 3b). 20% ethyl acetate 80% hexane eluent afforded 0.144 g (17% yield) of colorless oil. ^{1}H NMR ($CDCl_3$): δ (ppm) 0.82 (t, 3H), 1.21−1.61 (br, 41H), 2.01 (q, 4H), 3.29 (d, 2H), 3.41 (t, 2H), 3.50−3.71 (br, 16H) 4.98 (m, 4H), 5.82 (m, 2H). ^{13}C NMR ($CDCl_3$): δ (ppm) 14.21, 22.78, 25.95, 26.92, 29.12, 29.33, 29.68, 29.79, 29.82, 30.26, 31.53, 31.87, 33.98, 38.31, 70.26, 70.57, 70.78, 70.81, 70.83, 71.71, 74.98, 114.25, 139.33. ESI/HRMS: $[M + NH_4]^+$ calcd for $NH_4C_{38}H_{74}O_5$, 628.5875; found 628.5887. Anal. (CH) calcd for $C_{38}H_{74}O_5$: C, 74.70; H, 12.21. Found: C, 74.84; H, 12.36.

2-(10-Undecenyl)-12-tridecenyl-1-tetra(ethylene glycol) Mono-*n*-tetradecyl Ether (9,9TEGOC$_{14}$, 3c). 20% ethyl acetate and 80% hexane eluent afforded 0.400 g (34% yield) of colorless oil. ^{1}H NMR ($CDCl_3$): δ (ppm) 0.82 (t, 3H), 1.21−1.61 (br, 57H), 2.01 (q, 4H), 3.29 (d, 2H), 3.41 (t, 2H), 3.50−3.71 (br, 16H) 4.98 (m, 4H), 5.82 (m, 2H). ^{13}C NMR ($CDCl_3$): δ (ppm) 14.29, 22.88, 26.31, 27.03, 29.16, 29.36, 29.55, 29.71, 29.82, 29.85, 29.87, 30.29, 31.57, 32.13, 34.01, 38.35, 70.29, 70.60, 70.79, 70.84, 70.86, 71.75, 75.01, 114.27, 139.40. ESI/HRMS: $[M + NH_4]^+$ calcd for $NH_4C_{38}H_{74}O_5$, 628.5875; found 628.5887. Anal. (CH) calcd for $C_{38}H_{74}O_5$: C, 74.70; H, 12.21. Found: C, 74.84; H, 12.36.

General Procedure for ADMET Polymerizations. Monomers were dried under vacuum at 80 °C for 48 h prior to polymerization and subsequently transferred to a 50 mL round-bottom flask equipped with a magnetic stir bar. Grubbs first generation catalyst (300:1 monomer:catalyst ratio) was added, and the flask was stirred under vacuum at 45 °C for 4 days. Polymerizations were quenched with ethyl vinyl ether (5 drops in degassed toluene), precipitated into cold, acidic methanol to remove catalyst residue, and isolated as adhesive gums.

Polymerization of 2-(10-Undecenyl)-12-tridecenyl-1-tetra-(ethylene glycol)methenylpyrene (TEGOPy21u, 4a). ^{1}H NMR ($CDCl_3$): δ (ppm) 1.21−1.52 (br, 33H), 2.01 (q, 4H), 3.29 (d, 2H), 3.50−3.75 (br, 12H), 5.28 (s, 2H), 5.35 (m, 2H), 7.61−8.79 (m, 4H), 8.13−8.20 (m, 4H), 8.37 (d, 1H). ^{13}C NMR ($CDCl_3$): δ (ppm) 27.05, 27.46, 29.46, 29.35, 29.59, 29.78, 29.92, 30.02, 30.35, 31.57, 32.86, 38.33, 69.73, 70.54, 70.76, 70.83, 70.87, 70.95, 72.05, 74.96, 123.75, 124.64, 124.93, 125.13,, 125.33, 125.38, 126.10, 127.23, 127.57, 127.60, 127.84, 129.60, 130.08 (cis olefin), 130.53 (trans olefin), 131.03, 131.44, 131.47, 131.62. IR (ν, cm^{-1}): 2923, 2853, 1464, 1350, 1260, 1115, 967, 846, 802, 721. GPC (THF vs polystyrene standards): $M_w = 80\,300$; PDI (M_w/M_n) = 1.90.

Polymerization of 2-(10-Undecenyl)-12-tridecenyl-1-tetra-(ethylene glycol) Mono-*n*-hexyl Ether (TEGOHex21u, 4b). ^{1}H NMR ($CDCl_3$): δ (ppm) 0.82 (t, 3H), 1.21−1.61 (br, 41H), 2.01 (q, 4H), 3.29 (d, 2H), 3.41 (t, 2H), 3.50−3.71 (br, 16H), 5.35 (m, 2H). ^{13}C NMR ($CDCl_3$): δ (ppm) 14.26, 22.83, 25.99, 27.08, 29.49,

Scheme 1. Synthesis of Polyethylene with Precisely Placed Amphiphilic Branches[a]

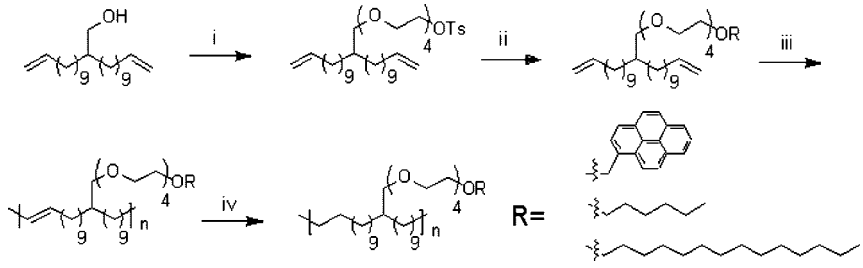

[a] Conditions: (i) NaH, tetra(ethylene glycol) di-*p*-tosylate, DMF; (ii) NaH, ROH, DMF; (iii) Grubbs' first generation catalyst, 45 °C, vacuum; (iv) TSH, TPA, *o*-xylene, 140 °C.

29.83, 29.97, 30.36, 31.61, 31.91, 32.87, 38.38, 70.29, 70.60, 70.86, 71.63, 75.06, 130.09 (cis olefin), 130.55 (trans olefin). IR (ν, cm^{-1}): 2923, 2853, 1464, 1350, 1260, 1115, 967, 846, 802, 721. GPC (THF vs polystyrene standards): M_w = 84 800; PDI (M_w/M_n) = 1.98.

Polymerization of 2-(10-Undecenyl)-12-tridecenyl-1-tetra-(ethylene glycol) Mono-*n*-tetradecyl Ether (TEGOC$_{14}$21u, 4c). ^{1}H NMR ($CDCl_3$): δ (ppm) 0.82 (t, 3H), 1.21−1.61 (br, 57H), 2.01 (q, 4H), 3.29 (d, 2H), 3.41 (t, 2H), 3.50−3.71 (br, 16H), 5.35 (m, 2H). ^{13}C NMR ($CDCl_3$): δ (ppm) 14.29, 22.88, 26.31, 27.03, 29.16, 29.36, 29.55, 29.71, 29.82, 29.85, 29.87, 30.29, 31.57, 32.13, 34.01, 38.35, 70.29, 70.61, 70.79, 70.84, 70.86, 71.76, 75.01, 130.08 (trans olefin), 130.54 (trans olefin). IR (ν, cm^{-1}): 2923, 2853, 1464, 1350, 1260, 1115, 967, 846, 802, 721. GPC (THF vs polystyrene standards): M_w = 61 900; PDI (M_w/M_n) = 1.71.

General Procedure for the Hydrogenation of Unsaturated Polymers. Unsaturated polymers were dissolved in dry *o*-xylene. *p*-Toluenesulfonyl hydrazide (TSH) and tripropylamine (TPA) were added with stirring (3 equiv each). The resulting solution was refluxed for 3−4 h while monitoring nitrogen evolution with a bubbler. When gas evolution ceased, the solution was cooled to room temperature, an additional 3 equiv of TSH and TPA was added, and the solution was refluxed for another 3 h. The solutions were then concentrated to one-half of the original volume and precipitated into cold, acidic methanol. The polymers were isolated as elastic, adhesive gums.

TEGOPy21 (5a). ^{1}H NMR ($CDCl_3$): δ (ppm) 1.21−1.52 (br, 41H), 3.29 (d, 2H), 3.50−3.75 (br, 12H), 5.28 (s, 2H), 7.61−8.79 (m, 4H), 8.13−8.20 (m, 4H), 8.37 (d, 1H). ^{13}C NMR ($CDCl_3$): δ (ppm) 27.05, 29.96, 30.02, 30.35, 31.59, 38.34, 69.76, 70.56, 70.78, 70.85, 70.87, 70.97, 72.05, 74.97, 123.75, 124.64, 124.95, 125.15,, 125.33, 125.38, 126.10, 127.23, 127.57, 127.61, 127.84, 129.60, 131.05, 131.44, 131.48, 131.66. IR (ν, cm^{-1}): 2923, 2853, 1464, 1350, 1260, 1115, 846, 802, 721. GPC (THF vs polystyrene standards): M_w = 60 400; PDI (M_w/M_n) = 1.93.

TEGOHex21 (5b). ^{1}H NMR ($CDCl_3$): δ (ppm) 0.82 (t, 3H), 1.21−1.61 (br, 49H), 3.29 (d, 2H), 3.41 (t, 2H), 3.50−3.71 (br, 16H). ^{13}C NMR ($CDCl_3$): δ (ppm) 14.28, 22.85, 25.99, 27.07, 29.83, 29.97, 30.38, 31.58, 31.93, 38.35, 70.29, 70.60, 70.84, 70.86, 71.77, 75.02. IR (ν, cm^{-1}): 2923, 2853, 1464, 1350, 1260, 1115, 846, 802, 721. GPC (THF vs polystyrene standards): M_w = 79 200; PDI (M_w/M_n) = 1.78.

TEGOC$_{14}$21 (5c). ^{1}H NMR ($CDCl_3$): δ (ppm) 0.82 (t, 3H), 1.21−1.61 (br, 65H), 3.29 (d, 2H), 3.41 (t, 2H), 3.50−3.71 (br, 16H), 5.35 (m, 2H). ^{13}C NMR ($CDCl_3$): δ (ppm) 14.29, 22.88, 26.31, 27.03, 29.55, 29.71, 29.82, 29.87, 29.97, 30.35, 31.60, 32.13, 38.38, 70.28, 70.61, 70.86, 71.76, 75.01. IR (ν, cm^{-1}): 2923, 2853, 1464, 1350, 1260, 1115, 846, 802, 721. GPC (THF vs polystyrene standards): M_w = 65 800; PDI (M_w/M_n) = 1.76.

Synthesis and Structural Analysis

Scheme 1 describes the synthesis of these unique materials. First, diene alcohol **1** (prepared as previously described[25]) is attached to the PEG branch via Williamson etherification with tetra(ethylene glycol) di-*p*-tosylate. Disubstitution is avoided using careful stoichiometry. The hydrophobic end group is then attached to **2** with a second Williamson by using the appropriate alcohol. This synthetic method is general and can potentially be applied to prepare an array of ADMET monomers and subsequent polymers having a variety of functional groups separated from the PE backbone by a PEG spacer. Monomers **3a**−**c** are polymerized in the bulk at 45 °C under high vacuum using Grubbs' first generation catalyst to afford the unsaturated ADMET polymers **4a**−**c**. Subsequent hydrogenation with *p*-toluenesulfonyl hydrazide results in the final fully saturated polymers **5a**−**c**.

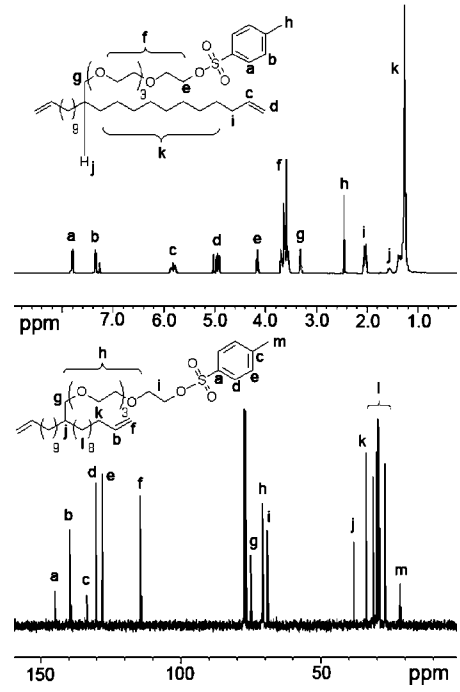

Figure 1. ^{1}H and ^{13}C NMR spectra of 9,9TEGOTs (**2**).

For simplicity, a systematic nomenclature has been adopted for these monomers and polymers. Monomers are given the prefix "99" to indicate the number of methylene carbons between the branch and the olefin, followed by the identity of the pendant group (TEGO for tetraethylene glycol and either Py, Hex, or C$_{14}$ for pyrene, *n*-hexyl, or *n*-tetradecyl). Polymers are named first for the identity of the pendant defect, followed by the branch frequency. Unsaturated polymers are denoted with the suffix "u". For example, monomer **3a** is named "99TEGOPy", polymer **4a** "TEGOPy21u", and polymer **5a** "TEGOPy21".

The ^{1}H and ^{13}C NMR spectra for 99TEGOTs (**2**) are shown in Figure 1. In the proton spectrum the tosyl end group is clearly identified by the two doublets at 7.32 and 7.72 ppm as well as the singlet at 2.45 ppm. The triplet at 4.16 ppm corresponds to the methylene protons adjacent to the tosyl group, shifted

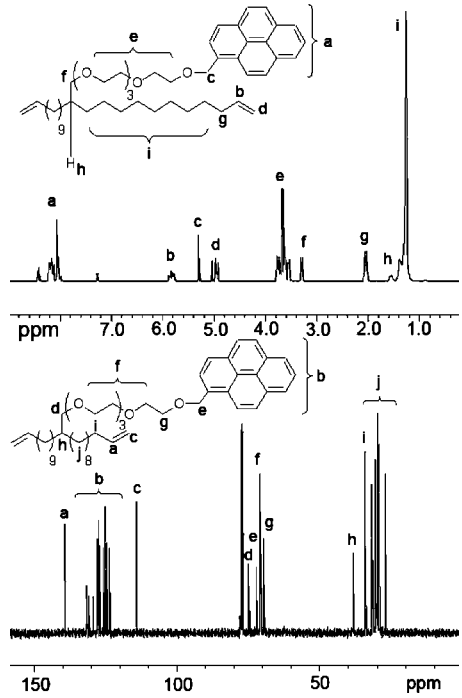

Figure 2. ^{1}H and ^{13}C NMR spectra of 9,9TEGOPy (**3a**).

downfield from the overlapping glycol proton signals which appear from 3.55 to 3.61 ppm. The doublet at 3.30 ppm corresponds to the methylene protons separating the glycol moiety from the backbone. The allylic protons display a quartet at 2.03 ppm, the central methine carbon shows a multiplet at 1.56 ppm, and the characteristic terminal olefin peaks are seen at 4.91 and 5.80 ppm. Finally, the remaining methylene protons of the diene main chain overlap into a single broad peak at 1.26 ppm. In the carbon spectra for 99TEGOTs the resonances for the tosyl group are seen at 144.92, 133.33, 129.99, and 128.18 ppm (aromatic carbons) and 21.83 ppm (methyl carbon). Terminal olefin signals appear at 114.28 and 139.43 ppm, the methylene carbon connecting the branch to the backbone appears at 75.01 ppm, and the glycol carbons overlap from 70.58 to 70.97 ppm. The glycol carbons closest to the tosyl group appear at 68.90 ppm, the central methine carbon is at 38.32 ppm, and the allylic carbons are at 34.01 ppm. The remaining resonances for the internal methylene carbons appear from 27 to 32 ppm and are all individually resolved. This highlights the need for thorough ^{13}C analysis in the ADMET synthesis of precise polyolefins because simply investigating the ^{1}H spectra can lead to ambiguities due to overlapping resonances.

The ^{1}H and ^{13}C NMR spectra of 99TEGOPy (**3a**) are shown in Figure 2. In the proton spectrum the aromatic pyrene protons appear from 8.02 to 8.43 ppm. The methylene protons between the pyrene and glycol branch appear as a singlet at 5.30 ppm. The resonances for the glycol region, terminal olefin, allylic, and aliphatic protons remain mostly unchanged compared to the ^{1}H spectrum of 9,9TEGOTs. The case is similar for the carbon spectrum of 9,9TEGOPy. The aromatic pyrene carbons appear from 123.74 to 131.61 ppm, and the methylene carbon between the pyrene and glycol moieties is seen at 72.04 ppm. As in the proton spectrum, the terminal olefin, allylic, and aliphatic carbons remain mostly unchanged compared to the carbon spectrum of 9,9TEGOTs.

Figures 3 and 4 show the ^{1}H and ^{13}C NMR spectra of 9,9TEGOHex (**3b**) and 9,9TEGOC$_{14}$ (**3c**). In the proton spectra the *n*-hexyl and *n*-tetradecyl methyl end groups appear at 0.87 ppm, and the methylene protons adjacent to the glycol portion of the branch appear as triplets at 3.44 ppm. The rest of the

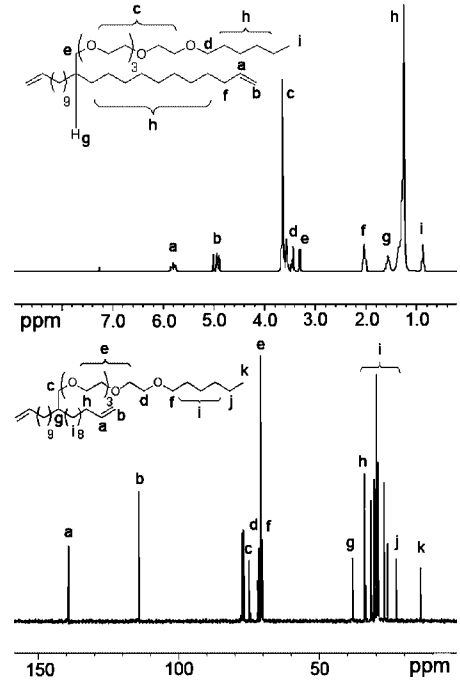

Figure 3. ^{1}H and ^{13}C NMR spectra of 9,9TEGOHex (**3b**).

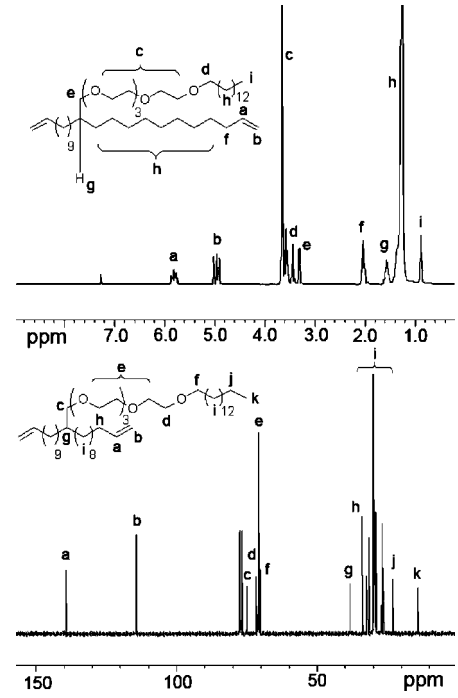

Figure 4. ^{1}H and ^{13}C NMR spectra of 9,9TEGOC14 (**3c**).

n-hexyl protons overlap with the internal methylene protons of the diene main chain. The remaining resonances are unchanged as described in the previous example. The carbon spectra for these monomers are nearly identical except for the aliphatic regions, which are complicated by the overlapping diene main chain and aliphatic branch carbon resonances.

An expanded view of the aliphatic regions in the ^{13}C NMR spectra of 9,9TEGOHex, 9,9TEGOC$_{14}$, and 9,9TEGOPy is shown in Figure 5. Comparing 9,9TEGOPy to the two monomers with aliphatic branch end groups allows the resonances for the diene main chain to be separated from the aliphatic end group resonances. Still, particularly in the case of 9,9TEGOC$_{14}$, the number of overlapping resonances greatly complicates the interpretation of this region.

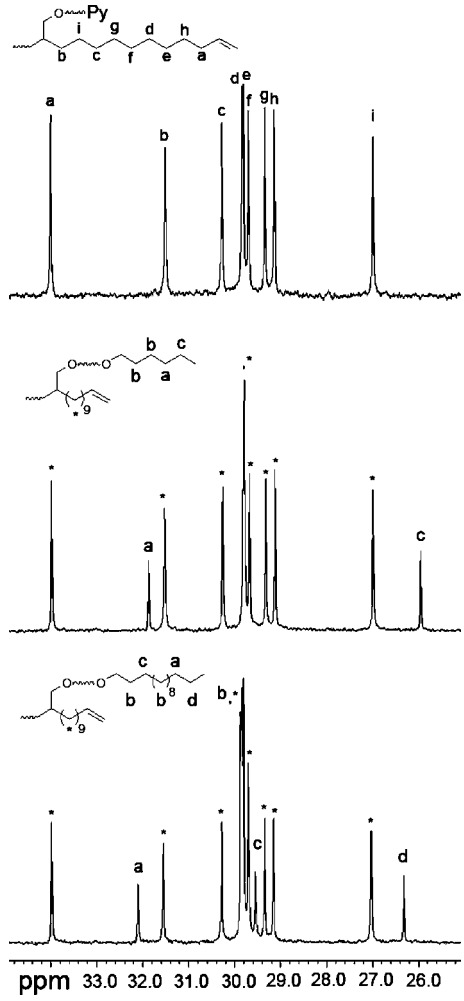

Figure 5. Expansion of the aliphatic regions of the ^{13}C spectra of 99TEGOPy, 99TEGOHex, and 9,9TEGOC$_{14}$ (**3a**−**c**).

The progression from diene monomer through unsaturated polymer to saturated polymer (monitored by ^{1}H and ^{13}C NMR) is shown in Figure 6 for 9,9TEGOC$_{14}$ (**3c**) through TEGOC$_{14}$21 (**5c**) (arbitrarily chosen as an example). Polymerization to **4c** results in convergence of the terminal olefin signals in the monomer spectrum to a single peak for internal olefin seen in both the ^{1}H and ^{13}C spectra. Hydrogenation results in the complete elimination of any olefin signal in either the proton or the carbon spectra. The appearance of only the resonances predicted by the fundamental repeat unit confirm the absence of side reactions and structural irregularities, again highlighting the effectiveness of ADMET chemistry in the synthesis of pristine, highly regular polymer structures.

Molecular weight data (GPC in THF vs polystyrene standards are displayed in Table 1.

Thermal Analysis

The DSC data for the new polymers are presented in Table 2. The polymers exhibit remarkably different thermal behavior, a clear indication that changing the graft end group moiety has significant effects on the morphology of these systems. The difference in behavior between the saturated and unsaturated polymers is also significant, emphasizing the role of the PE backbone on the crystallization in these materials.

The DSC profiles for TEGOPy21 and TEGOPy21u are shown in Figure 7. The heating and cooling curves show that the saturation of the backbone allows for crystallization to occur, while the unsaturated polymer remains completely amorphous.

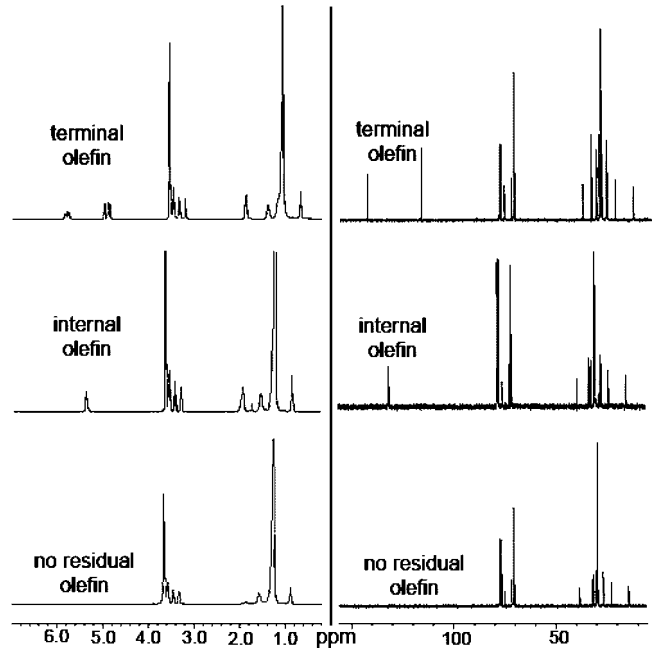

Figure 6. Progression from monomer **3c** to saturated polymer **5c** monitored by NMR.

Table 1. Molecular Weight Data

polymer	M_n[a] (kg/mol)	M_w[a] (kg/mol)	PDI[b]
TEGOPy21u (**4a**)	42.2	80.3	1.9
TEGOPy21 (**5a**)	31.2	60.4	1.93
TEGOHex21u (**4b**)	42.8	84.8	1.98
TEGOHex21 (**5b**)	44.4	79.2	1.78
TEGOC$_{14}$21u (**4c**)	36.2	61.9	1.71
TEGOC$_{14}$21 (**5c**)	37.3	65.8	1.76

[a] GPC vs polystyrene standards. [b] M_w/M_n.

Table 2. DSC Data

polymer	T_g (°C)	ΔC_p (J/(g °C))	T_m (°C)	ΔH_m (J/g)	T_c (°C)	ΔH_c (J/g)
TEGOPy21u (**4a**)	−36	0.76	n/a	n/a	n/a	n/a
TEGOPy21 (**5a**)	−21	0.36	9	24	−12	25
TEGOHex21u (**4b**)	−76	0.49	−13	21	−54	21
TEGOHex21 (**5b**)	n/a	n/a	−374	827	−4	28
TEGOC$_{14}$21u (**4c**)	n/a	n/a	−3	50	−7	51
TEGOC$_{14}$21 (**5c**)	n/a	n/a	23	71	17	72

This suggests that the pendant defect is not involved in the crystallization and therefore must be excluded from the crystal. The T_g of the saturated polymer is also slightly increased compared to the unsaturated analogue, an indication that segmented motion of the grafts is restricted by the crystallinity.

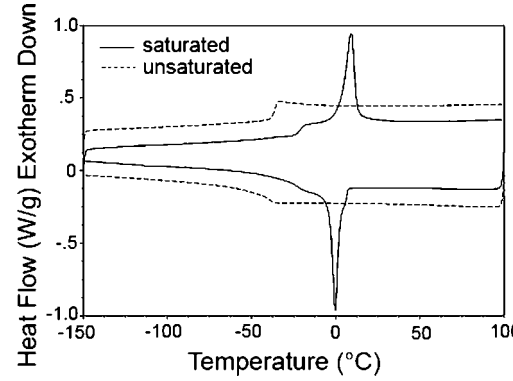

Figure 7. DSC heating and cooling traces for TEGOPy21u (**4a**) and TEGOPy21 (**5a**).

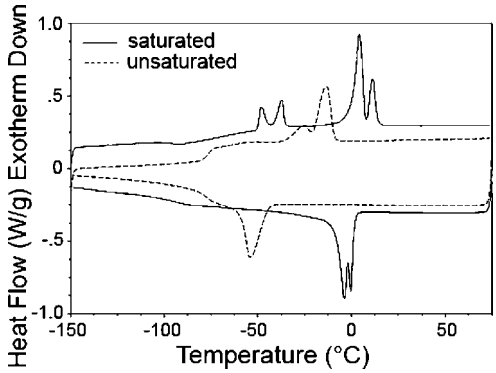

Figure 8. DSC heating and cooling traces for TEGOHex21u (**4b**) and TEGOHex21 (**5b**).

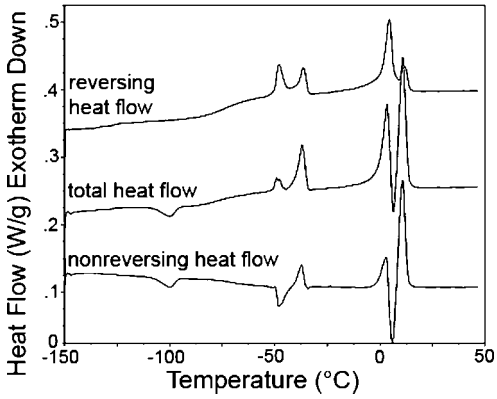

Figure 9. MDSC heating trace of TEGOHex21 (**5b**).

The completely amorphous behavior of TEGOPy21u is an interesting result, considering that previous reported unsaturated ADMET polymers with the same distribution of pendant functionality are semicrystalline.[16–18] The lack of crystallinity in TEGOPy21u as well as the significantly depressed melting point for the saturated analogue compared to our previous ADMET amphiphilic copolymers[30] is a result of pyrene aggregation impeding the backbone crystallization. This is confirmed by pyrene excimer formation seen in the fluorescence spectra for both the unsaturated and saturated polymers (see Supporting Information).

The DSC curves for TEGOHex21 and TEGOHex21u are shown in Figure 8. The difference in behavior between the saturated and unsaturated polymers is especially interesting in this pair. The unsaturated polymer is semicrystalline with a melting endotherm at −13 °C. There is significant amorphous content to this material as well, indicated by the distinct T_g at −76 °C. The heating and cooling profiles are typical for unsaturated ADMET polymers. The thermal behavior of the saturated analogue is completely different, however. A single, bimodal crystallization at −4 °C is witnessed on cooling. Upon heating a small exotherm is barely observed at −91 °C, followed by a bimodal melting endotherm with peaks at −48 and −37 °C. A second bimodal melting endotherm occurs with peaks at 4 and 11 °C.

The complex behavior of TEGOHex21 was further investigated by MDSC, which provides increased sensitivity compared to traditional DSC and allows for resolution of overlapping transitions.[31–34] The MDSC heating traces are shown in Figure 9. In the nonreversing and total heat flow signals the cold crystallization event, barely perceptible in Figure 8, is clearly visible. This is followed by the first bimodal melting endotherm, which is observed in all three signals. In the nonreversing signal this transition is first exothermic and then endothermic, indicating that the bimodal melt is actually the result of a melting and crystalline perfection mechanism.[31] The same is true for the higher temperature bimodal endotherm; clear exothermic activity in both the total and nonreversing signals indicates melting and crystalline perfection. Because the melting enthalpy of this higher temperature peak (21 J/g) matches the enthalpy of crystallization (21 J/g) and also because its melting temperature and enthalpy (4 °C and 27 J/g) are in good agreement with with those of TEGOPy21 (9 °C and 24 J/g), it can be concluded that this behavior is a result of crystallization of the backbone excluding the pendant branch. The backbone crystallizes during cooling. Then during subsequent heating, the excluded branches gain sufficient mobility to self-crystallize, noted by the exotherm at −100 °C. The pendant crystals then melt at about −50 °C, followed by the melting of the backbone crystals.

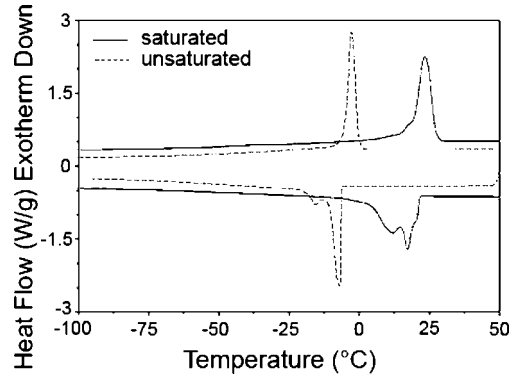

Figure 10. DSC heating and cooling traces for $TEGOC_{14}21u$ (**4c**) and $TEGOC_{14}21$ (**5c**).

The thermal behavior of $TEGOC_{14}21u$ and $TEGOC_{14}21$ (Figure 10) differs significantly from the previous two examples. Both polymers exhibit extremely sharp melting transitions at temperatures much higher than the other polymers in this family. This deviates from the well-known trend for ADMET polymers, which show a decrease in T_m and ΔH_m as the defect size increases. For $TEGOC_{14}21u$ and $TEGOC_{14}21$, the increase in pendant group length results in marked increases in both melting temperature and enthalpy. Further, no T_g is observed in either the saturated or unsaturated analogues, indicating the absence of amorphous content for these polymers. Thus, the long alkyl chains must also be crystallizing. Since there is only one melting peak, the C_{14} chain must be long enough to extend back into the crystallizing PE backbone, forming a single crystallized region.

Conclusions

The synthesis of polyethylene with precise placement of amphiphilic grafts has been achieved. These polymers feature PEG grafts attached to the polyolefin backbone with different hydrophobic groups affixed to the end of the PEG chains. These structural differences induce significant changes in the thermal behavior of the corresponding materials. When the graft end group is a pyrene moiety, the polyolefin backbone crystallizes, excluding the pendant branch. When the end group is changed to an *n*-hexyl chain, the branches and the backbone crystallize separately, forming two different crystalline regions. Extending this end group from an *n*-hexyl to an *n*-tetradecyl chain allows the branches and backbone to crystallize together, resulting in the inclusion of the branch within the PE crystal. This material breaks the well-known trend for ADMET polymers, which show a decrease in T_m and ΔH_m as the defect size increases. Most importantly, we have demonstrated that a pendant group can be intentionally excluded from the crystallized polyethylene backbone and induced to self-interact. This displays the promise

this architecture could have in advanced applications such as membrane technologies or polymer electrolytes.

Acknowledgment. The authors thank the National Science Foundation (NSF) and the Army Research Office (ARO) for financial support. We also thank Materia, Inc., for the catalyst, Dr. Cristina Dancel for assistance with HRMS of monomers, and Dr. Katsu Ogawa and Dr. Stefan Ellinger for assistance with UV−vis and fluorescence measurements.

Supporting Information Available: UV−vis and fluorescence spectra for the pyrene-labeled polymers described in this article. This material is available free of charge via the Internet at http://pubs.acs.org.

References and Notes

(1) Rodriguez-Hernandez, J.; Checot, F.; Gnanou, Y.; Lecommandoux, S. *Prog. Polym. Sci.* **2005**, *30* (7), 691–724.
(2) Rider, D. A.; Cavicchi, K. A.; Power-Billard, K. N.; Russell, T. P.; Manners, I. *Macromolecules* **2005**, *38* (16), 6931–6938.
(3) Kim, Y.; Pyun, J.; Frechet, J. M. J.; Hawker, C. J.; Frank, C. W. *Langmuir* **2005**, *21* (23), 10444–10458.
(4) Allcock, H. R.; Powell, E. S.; Chang, Y.; Kim, C. *Macromolecules* **2004**, *37* (19), 7163–7167.
(5) Park, C.; Yoon, J.; Thomas, E. L. *Polymer* **2003**, *44* (22), 6725–6760.
(6) Yu, Z.; Liu, L. *J. Biomater. Sci., Polym. Ed.* **2005**, *16* (8), 957–971.
(7) Wang, F.; Bronich, T. K.; Kabanov, A. V.; Rauh, R. D.; Roovers, J. *Bioconjugate Chem.* **2005**, *16* (2), 397–405.
(8) Huang, W.; Zhou, Y.; Yan, D. *J. Polym. Sci., Part A: Polym. Chem.* **2005**, *43* (10), 2038–2047.
(9) Cheng, Z.; Zhu, X.; Kang, E. T.; Neoh, K. G. *Langmuir* **2005**, *21* (16), 7180–7185.
(10) Schmalz, H.; Knoll, A.; Muller, A. J.; Abetz, V. *Macromolecules* **2002**, *35* (27), 10004–10013.
(11) Hillmyer, M. A.; Bates, F. S. *Macromolecules* **1996**, *29* (22), 6994–7002.
(12) Fu, G. D.; Phua, S. J.; Kang, E. T.; Neoh, K. G. *Macromolecules* **2005**, *38* (7), 2612–2619.
(13) Tian, H. Y.; Deng, C.; Lin, H.; Sun, J.; Deng, M.; Chen, X.; Jing, X. *Biomaterials* **2005**, *26* (20), 4209–4217.
(14) Vlcek, P.; Otoupalova, J.; Sikora, A.; Kriz, J. *Macromolecules* **1995**, *28* (21), 7262–7265.
(15) Singh, R.; Verploegen, E.; Hammond, P. T.; Schrock, R. R. *Macromolecules* **2006**, *39* (24), 8241–8249.
(16) Berda, E. B.; Baughman, T. W.; Wagener, K. B. *J. Polym. Sci., Part A: Polym. Chem.* **2006**, *44* (17), 4981–4989.
(17) Baughman, T. W.; Wagener, K. B. *Adv. Polym. Sci.* **2005**, *176* (Metathesis Polymerization), 1–42.
(18) Lehman, S. E.; Wagener, K. B. ADMET Polymerization. In *The Handbook of Metathesis*; Grubbs, R. H., Ed.; Wiley: New York, 2003; Vol. *3*.
(19) Sworen, J. C.; Wagener, K. B. *Macromolecules* **2007**, *40* (13), 4414–4423.
(20) Lehman, S. E.; Wagener, K. B.; Baugh, L. S.; Rucker, S. P.; Schulz, D. N.; Varma-Nair, M.; Berluche, E. *Macromolecules* **2007**, *40* (8), 2643–2656.
(21) Boz, E.; Nemeth, A. J.; Ghiviriga, I.; Jeon, K.; Alamo, R. G.; Wagener, K. B. *Macromolecules* **2007**, *40* (18), 6545–6551.
(22) Boz, E.; Nemeth; Alexander, J.; Alamo, R. G.; Wagener, K. B. *Adv. Synth. Catal.* **2007**, *349* (1−2), 137–141.
(23) Baughman, T. W.; Chan, C. D.; Winey, K. I.; Wagener, K. B. *Macromolecules* **2007**, *40* (18), 6564–6571.
(24) Boz, E.; Wagener, K. B.; Ghosal, A.; Fu, R.; Alamo, R. G. *Macromolecules* **2006**, *39* (13), 4437–4447.
(25) Sworen, J. C.; Smith, J. A.; Berg, J. M.; Wagener, K. B. *J. Am. Chem. Soc.* **2004**, *126* (36), 11238–11246.
(26) Watson, M. D.; Wagener, K. B. *Macromolecules* **2000**, *33* (24), 8963–8970.
(27) Smith, J. A.; Brzezinska, K. R.; Valenti, D. J.; Wagener, K. B. *Macromolecules* **2000**, *33* (10), 3781–3794.
(28) Baughman, T. W.; vanderAa, E.; Wagener, K. B. *Macromolecules* **2006**, *39* (20), 7015–7021.
(29) Baughman, T. W.; Sworen, J. C.; Wagener, K. B. *Macromolecules* **2006**, *39* (15), 5028–5036.
(30) Berda, E. B.; Lande, R. E.; Wagener, K. B. *Macromolecules* **2007**, *40*, 8547–8552.
(31) Shieh, Y.-T.; Liu, G.-L. *J. Polym. Sci., Part B: Polym. Phys.* **2007**, *45* (4), 466–474.
(32) Wunderlich, B. *J. Therm. Anal. Calorim.* **2006**, *85* (1), 179–187.
(33) Schawe, J. E. K. *Thermochim. Acta* **1997**, *304−305*, 111–119.
(34) Jones, K. J.; Kinshott, I.; Reading, M.; Lacey, A. A.; Nikolopoulos, C.; Pollock, H. M. *Thermochim. Acta* **1997**, *304−305*, 187–199.

MA800616H